# STABILITY OF FILM FLOW OVER A SUBSTRATE WITH RECTANGULAR TRENCHES FORMING AIR INCLUSIONS

**D. Pettas[1], G. Karapetsas[1], J. Tsamopoulos[1,*]**
[1] Department of Chemical Engineering, University of Patras, Rio, Greece
[2] Department of Chemical Engineering, Aristotle University of Thessaloniki, Thessaloniki, Greece
(*tsamo@chemeng.upatras.gr)

## ABSTRACT

In this paper, we study the linear hydrodynamic stability of a film of Newtonian fluid flowing down an inclined, solid substrate featuring periodic rectangular trenches. Due to the geometric characteristics of the substrate, the film fails to completely wet the topography creating an enclosure of air inside the cavity. The inner interface forms two three-phase contact lines and supports a widely varying amount of liquid under different physical and geometrical conditions [1, 2]. The exact liquid configuration is determined by employing the Galerkin/finite element method to solve the two-dimensional Navier–Stokes equations at steady state, combined with an elliptic grid generation in order to take into account the free surface deformations. The generalized eigenvalue problem is solved using Arnoldi's algorithm, in a Newton-like implementation to calculate faster the critical conditions for the onset of the instability, while we employ Floquet theory[3] to predict the stability of periodic disturbances of arbitrary wavelengths, which in general are larger than the periodicity of the substrate. Numerical simulations highlight the effect of inertia, viscous and capillary forces along with the substrate wettability and orientation with respect to gravity and the geometric characteristics of the substrate on the stability of the fluid flow. Due to the existence of triple contact points, multiple steady states may occur which are analyzed for their stability. Interestingly, it is shown that the presence of air inclusions in the trenches act as a damper preventing the disturbances on the outer free surface of the film.

## INTRODUCTION

Steady film flow of a Newtonian liquid over an inclined plane with variable topography is of great importance in various engineering applications with scales ranging from micro to macro. This is a basic model for coating and liquid film deposition processes, which is very widely used in fabrication of microelectronic components, gravure printing[4] and in heat or mass transfer operations (e.g., two-phase heat exchangers and adsorption or distillation columns using structured packings[5], falling film reactors and in many other applications[6]. In many of these applications, the substrates have some kind of structure, and the flow is typically driven by a body force (such as gravity or centrifugal force) or by the motion of the substrate. In practice, the substrates encountered are never completely flat since they may contain well-defined features in the form of sharp steps, trenches, pillars, corrugations, etc. while irregularities may also arise due to the presence of arrested drops and particles on the substrate. Besides thickness variations of the coated layer, the presence of these topographic features may also lead to air entrapment inside them under certain conditions, which may affect significantly the flow dynamics as well as the resulting coating quality of the solid surface.

Very recently, Varchanis *et al.* [2] developed an accurate and efficient numerical method to solve the steady thin film flow of a Newtonian film over a substrate with periodically features and examined new possible film arrangements. They found the existence of isolated multiple steady-state solutions, while the competition between capillary, viscous, and inertia forces gives rise to hydrodynamic hysteresis loops. The goal of the present study is to investigate the linear stability analysis of the obtained steady-state solutions to identify which flow configuration will prevail.

## PROBLEM FORMULATION

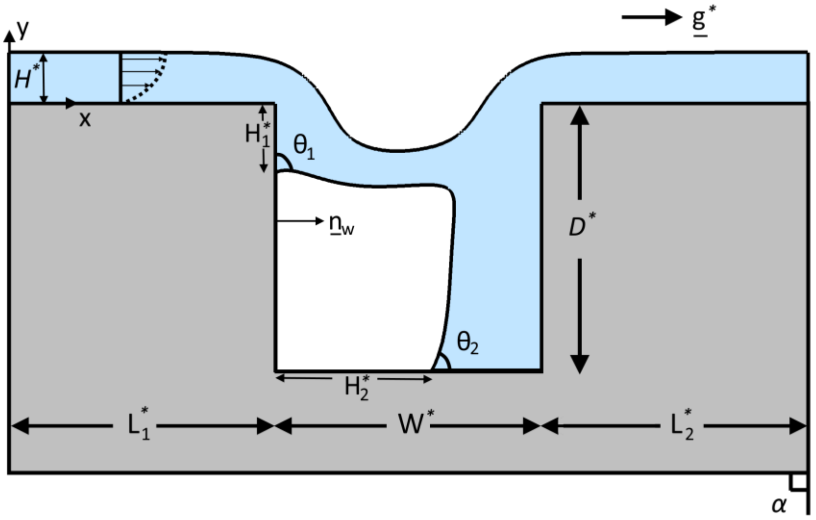


***Figure 1*** *Cross section of the film flowing over a rectangle trench with air inclusion at the upstream corner. The geometric parameters, the orientation of the substrate, the unit vector of the wall and the contact points angles are indicated, while the film thickness at the entrance is* $H^*$.

We consider as a model system the steady, two-dimensional film flow of a Newtonian fluid on a plane inclined with respect to gravity by an angle α and featuring a trench; imposing that $\alpha = 90^o$. The fluid is incompressible with constant density $\rho^*$, interfacial surface tension $\sigma^*$, and dynamic viscosity $\mu^*$. The film of thickness $H^*$is flowing over the topographic feature with a sudden expansion in the film flow cross-section located at distance $L_1^*$ from the entrance. The trench that is formed has depth $D^*$ and width $W^*$, while the distance from the sudden contraction to the exit is $L_2^*$, see Fig. 1. The primitive flow input is the volumetric flow rate per unit length normal to the film cross-section, $q^*$. The liquid may form with the solid an apparent contact angle $\theta$, which is the angle between $\boldsymbol{n}_w$, the unit normal vector to the solid wall, and the normal $\boldsymbol{n}$ to the visible free surface at a putative contact line. The flow is described using a Cartesian coordinate system with its origin located at the entrance of the flow domain, with the $x$-axis and $y$-axis in the direction parallel and normal to the wall at $x = 0$, respectively (see Fig. 1).

The flow is governed by the momentum and mass conservation equations, which under the Arbitrary Eulerian-Lagrangian (ALE) formulation in the dimensionless form are given by:

$$\rho^*(\partial \boldsymbol{u}^*/\partial t^* + (\boldsymbol{u}^* - \boldsymbol{u}_{\boldsymbol{m}}^*)\cdot\nabla\boldsymbol{u}^*) + \nabla P^* - \mu^*\,\nabla^2\boldsymbol{u}^* - \rho^*\boldsymbol{g}^* = \boldsymbol{0}\,,\ \nabla\cdot\boldsymbol{u}^* = \boldsymbol{0} \qquad (1)$$

where $\boldsymbol{u}^* = \left(u_x^*, u_y^*, u_z^*\right)^T$, $P^*$, denote the velocity, pressure fields, respectively, and $\boldsymbol{u}_m^* = \frac{\partial x^*}{\partial t^*}$ the velocity of the mesh nodes in the flow domain. We also define the unit gravity vector as $\boldsymbol{g}^* = g^*(\sin a\,, -\cos a)^T$.

Along with the two air-liquid interfaces, we apply a stress balance between capillary forces and stresses:

$$\boldsymbol{n}\cdot(-P^*\boldsymbol{I} + \boldsymbol{\tau}^*) = -\gamma^*\nabla_s\cdot\boldsymbol{n}, \qquad (2)$$

We also impose the kinematic condition:

$$\boldsymbol{n} \cdot (\boldsymbol{u}^* - \partial \boldsymbol{x}^*/\partial t^*) = 0, \tag{3}$$

while along the walls of the substrate, we impose the usual no-slip, no-penetration boundary conditions.

At the two intersections of the inner interface with the two trench walls, the following equations are imposed allowing the contact lines to move along the walls,

$$\boldsymbol{n}_{s1} \cdot \boldsymbol{n}_{w1} = \cos\theta_1, \tag{4}$$

$$\boldsymbol{n}_{s2} \cdot \boldsymbol{n}_{w2} = \cos\theta_2, \tag{5}$$

Additionally, we impose periodic boundary conditions in the velocity and stress field between the inflow and the outflow of the domain, assuming the steady flow has the same periodicity as the substrate structure (i.e., we assume that the steady solution is $L$-periodic)

$$\boldsymbol{u}^*|_{x=0} = \boldsymbol{u}^*|_{x=L}, \quad \boldsymbol{n} \cdot \left(-P^*\boldsymbol{I} + \boldsymbol{\tau}^*\right)\big|_{x=0} = \boldsymbol{n} \cdot \left(-P^*\boldsymbol{I} + \boldsymbol{\tau}^*\right)\big|_{x=L} \tag{6}$$

where $L^* = L_1^* + W^* + L_2^*$.

Finally, the film height at the entrance of the unit cell $H^*$ , is determined by requiring that the flow rate is constant.

$$q^* = \int_0^{H^*} u_x^* dy^* \tag{7}$$

As mentioned above, the base flow is steady, two-dimensional and is assumed to be $L$-periodic. We consider the stability of this steady flow subjected to infinitesimal *2D* disturbances. To this end, we map the perturbed physical domain $(x, y)$ to a known reference domain $(\eta, \xi)$. The variables are written in the computational domain and are decomposed into a part which corresponds to the base state solution and an infinitesimal disturbance using the following ansatz:

$$\begin{bmatrix} \boldsymbol{u} \\ P \\ x \\ y \end{bmatrix} (\eta, \xi, t) = \begin{bmatrix} \boldsymbol{u}_b \\ P_b \\ x_b \\ y_b \end{bmatrix} (\eta, \xi) + \delta \begin{bmatrix} \boldsymbol{u}'_d \\ P'_d \\ x'_d \\ y'_d \end{bmatrix} (\eta, \xi) e^{\lambda t}, \tag{8}$$

The first terms on the right-hand side of these equations represent the base solution, indicated by the subscript “$b$”, while the second ones are the perturbation, indicated by the subscript “$d$” while $\delta \ll 1$. Introducing eq. (8) in the weak form of the governing equations, we derive a linearized set of equations for the flow in the bulk and the corresponding boundary conditions. According to our ansatz, an exponential dependence on time is assumed; here $\lambda$ denotes the growth rate. If the calculated $\lambda$ turns out to have a positive real part, the disturbance grows with time, and therefore the corresponding steady state is unstable. The disturbances $\boldsymbol{u}'_d$, $P'_d$, $x'_d, y'_d$ are discretized employing finite element basis functions in the streamwise and spanwise directions.

For flows over periodically structured surfaces, the most unstable disturbance for the specific system may have a wavelength that exceeds the period of the domain. Thus, the most appropriate and efficient way to deal with this issue is to employ the Floquet-Bloch theory, which allows us to model the flow over a structured surface by considering the small periodic domain of the topography. According to Bloch’s theorem, it is sufficient to look for solutions such that the disturbances between the inflow and outflow of the unity cell are related to each other with the following expression

$$\left.\begin{bmatrix} \boldsymbol{u}'_d \\ P'_d \\ y'_d \end{bmatrix}\right|_{x=L} = \left.\begin{bmatrix} \boldsymbol{u}'_d \\ P'_d \\ y'_d \end{bmatrix}\right|_{x=0} e^{2\pi Q i} \tag{9}$$

$$\boldsymbol{n}\cdot\left(-P_d'\boldsymbol{I}+\boldsymbol{\tau}_p'\right)\Big|_{x=L} = \boldsymbol{n}\cdot\left(-P_d'\boldsymbol{I}+\boldsymbol{\tau}_p'\right)\Big|_{x=0} e^{2\pi\, Q\, i} \qquad (10)$$

Using this formulation, the unknown disturbances, $(\boldsymbol{u}_d', P_d', y_d')^T$, will be determined by imposing eq. (9,10) at the edges of the periodic domain, which enforces that for finite real values of $Q$ the disturbances will not be $L$-periodic. Disturbances with $Q = 0$ should be distinguished since in that case eq. (9) reduces to typical periodic boundary conditions, and thus this case corresponds to disturbances that have the same period or aliquots of the basic solution i.e. correspon,d to super-harmonic instabilities.

## RESULTS AND DISCUSSION

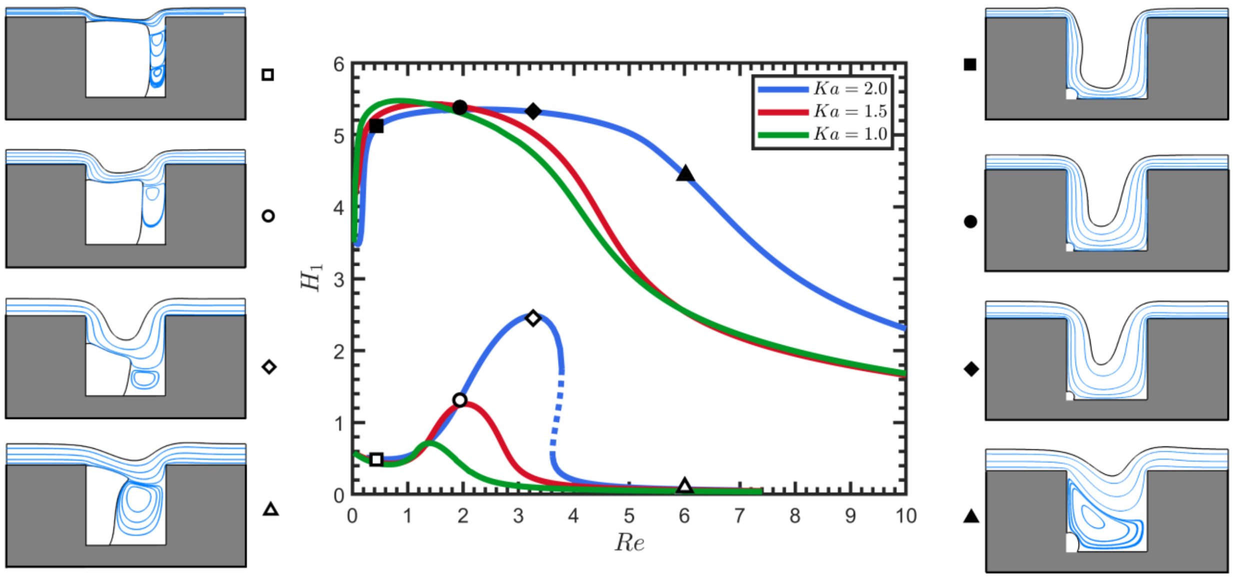


***Figure 2*** *Map of the steady-state solutions in terms of the wetting distance* $H_1^*/\sqrt{\frac{\rho^* g^*}{\sigma^*}}$ *for* $Ka = 1, 1.5, 2$, $\theta = 60^o$ *and* $\alpha = 90^o$ *for* $d = D^*/\sqrt{\rho^* g^*/\sigma^*} = 6$ *and* $w = W^*/\sqrt{\rho^* g^*/\sigma^*} = 6$. *The symbols in the solution families correspond to one of the flow patterns around the figure.*

We begin our discussion by presenting in Fig. 2 the wetting lengths $H_1^*$ as a function of Reynolds number, $Re = \rho^* q^* / \mu^*$, for various values of Kapitza number, $Ka = \gamma^* {\rho^*}^{1/3} {g^*}^{-1/3} {\mu^*}^{-4/3}$; in contrast with other dimensionless quantities that may arise in the problem, $Ka$ depends only on liquid properties such as surface tension, density and dynamic viscosity. At least two steady states coexist for every value of $Re$ where we performed simulations, composing two solution branches: a branch in which the flow profiles feature deep penetration of the liquid in the trench leading to almost full coating with a tiny air inclusion (this will be called the "upper" branch from now on) and a branch in which the liquid penetrates partially the trench forming a large air inclusion (this will be called the "lower" branch from now on). The insets in Fig. 2 represent the film arrangements with streamline patterns for $Ka = 2$.

First, we examine the lower branch following the change of the flow profile with increasing inertia or flow rate starting with $Re = 0.5$. We note that the wetting distance $H_1^*$ tends to increase until a maximum is reached. Then we can observe two successive turning points defining a hysteresis loop at about $Re_c \approx 3.9$, which resembles the hydrodynamic hysteresis that Kistler and Scriven[7] observed in the so-called teapot effect, and also the hydrodynamic hysteresis Pettas *et al.* [1] found when examining the flow of a liquid film over an inclined plane with a slit. At even higher flow rates, the contact line at the upstream wall tends to become pinned on the convex upstream corner, but the simulation ends before $H_1^* = 0$.

Second, examining the upper branch, we can see that the wetting penetration distance of contact lines at the upstream and bottom vary only slightly, always remaining near the upstream concave corner. On the other hand, the deformation amplitude of the outer interface, see insets that lie on the right side of Fig.2, is affected significantly by the change on the flow rate. Under creeping flow conditions, due to the high viscous forces, the free surface of the fluid nearly follows the shape of the bottom wall, while at high inertia the free surface tends to be flat since the film succeeds to overpass the trench.

In Fig. 2 presents the wetting distance $H_1^*$ for different liquids. In practice, the Kapitza number varies mainly due to the liquid viscosity, since surface tension and density of common liquids vary in much sorter range. For high viscosity liquids (small values of $Ka$), the hysteresis loop that is lied in the lower branch vanishes, which can be attributed to the balance of the capillary force with the viscous forces at the contact line position; the more viscous the liquid is the less the wetting penetration. Thus, the transition from creeping flow to inertia flow is smoother and takes place earlier.

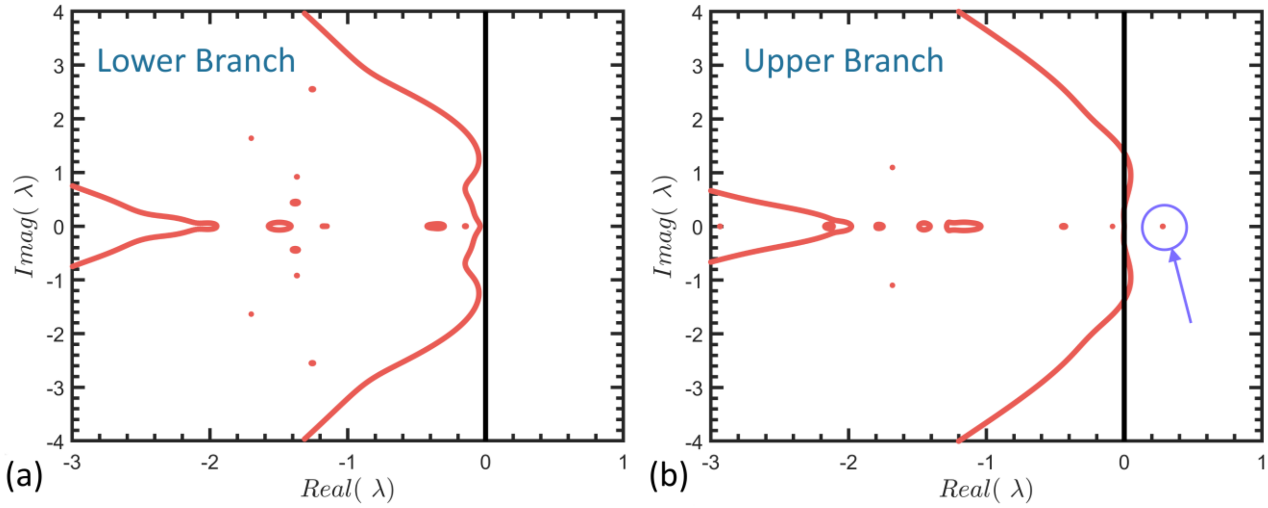


***Figure 3*** *Spectrum for a steady solution that lies in the (a) lower and (b) upper branch of the steady curves for* $Re = 2$, $Ka = 1.5$, $\theta = 60^o$ *and* $\alpha = 90^o$.

In Fig. 3 (a,b) we present the eigenspectrum for $Re = 2$ and $Ka = 1.5$ at the upper and lower branch of the steady curves, respectively, while the Floquet parameter "$Q$" varies in the range of $[0,1)$. In Fig. 3(a) the real part of all the calculated eigenvalues are negative indicating that at this value of $Re$ the steady state is stable under all possible values of $Q$. In contrast with the previous results, in Fig. 3(b) we present the eigenspectrum of a steady state that lies in the upper steady branch, which is unstable since there are some eigenmodes that have a positive real part. However, the special notation is given in the unstable eigenvalue that lies at $0.24 + 0i$, see the eigenvalue inside the circle in Fig. 3(b). This eigenvalue is real (the imaginary part of the eigenvalue is zero) indicating that the steady solution is globally unstable, since the disturbances monotonically increase with increasing time. Note that the real eigenvalue remains always positive for every value of $Re$ that we performed simulations indicating that the upper steady branch is unstable and therefore cannot be observed in experiments, while the corresponding eigenvector indicates that the air inclusion will collapse under the strong the capillary pressure field that arises.

## CONCLUSIONS

We carried out a theoretical analysis of the linear stability of a Newtonian liquid film flowing down an inclined solid substrate featuring periodic rectangular trenches. The analysis for the steady state flow revealed the existence of multiple steady-states for every value of $Re$ that we performed simulations. In the upper branch, the air inclusion is located near the upstream concave corner, while on the lower branch the air inclusion occupies a significant amount of trench space. Moreover, the competition of the inertial with viscous and capillary forces generates a hysteresis loop, which resembles the hydrodynamic hysteresis that Kistler and Scriven [7] observed in the so-called teapot effect. The linear stability, considering infinitesimal perturbations around this base state, predicts that the steady states that lies on the upper branch of the steady curves are unstable for all values of the Reynolds number, since there is a real eigenvalue with a positive value. Thus, this curve cannot be observed experimentally. On the lower branch, a robust stabilization of the fluid flow is presented since the inner interface acts as a damper which stabilizes mainly the long-wave disturbances. Interestingly, the critical $Re$ was calculated to be 20 times larger compared with the case of full coated substrate.

## ACKNOWLEDGMENTS

This work has been supported financially by the Hellenic Foundation for Research and Innovation (HFRI) and the General Secretariat for Research and Technology (GSRT), under grand agreement No 1743 and the LIMMAT foundation under the grant MuSiComPS. GK would also like to acknowledge the financial support from the Hellenic Foundation for Research and Innovation (HFRI) and the General Secretariat for Research and Technology (GSRT), under grant agreement No 792.

LIMMAT STIFTUNG
Bridging Worlds
H.F.R.I.
Hellenic Foundation for Research & Innovation
GSRT
GENERAL SECRETARIAT FOR RESEARCH AND TECHNOLOGY

## BIBLIOGRAPHY

[1] D. Pettas, G. Karapetsas, Y. Dimakopoulos, J. Tsamopoulos. J. Fluid Mech. 820 (2017) 5.
[2] S. Varchanis, Y. Dimakopoulos, J. Tsamopoulos. Phys. Rev. Fluids 2(12) (2017) 1-28.
[3] Y. Trifonov. Phys. Fluids 26 (2014) 114101.
[4] X. Yin, S. Kumar. Chem. Eng. Sci. 61 (2006) 497-499.
[5] K. Argyriadi, M. Vlachogiannis, V. Bontozoglou. Phys. Fluids 18 (2006) 012102.
[6] R.V. Craster, O. K. Matar. Rev. Mod. Phys. 81 (2009) 1131.
[7] S. F. Kistler, L.E. Scriven. J. Fluid Mech. 263 (1994) 19.